Universiteit Utrecht

External light-trapping for solar cells using a 3D-printed parabolic concentrator array

June 15, 2014

Abstract

Reflection of light is a major efficiency loss in solar cells. Most optical absorption enhancement methods in solar cells increase surface recombination. An array of external light-traps can increase optical absorption without deteriorating cell quality. We fabricated square, hexagonal and circular parabolic light-traps for solar cells. We performed electrical and spectral response measurements on an organic photovoltaic cell, with and without 3D-printed light-traps. The external quantum efficiency of the cell shows that for almost all wavelengths of interest, the traps improve the efficiency of the solar cell. We made a 2x2 array of square traps that improves the efficiency of the cell.

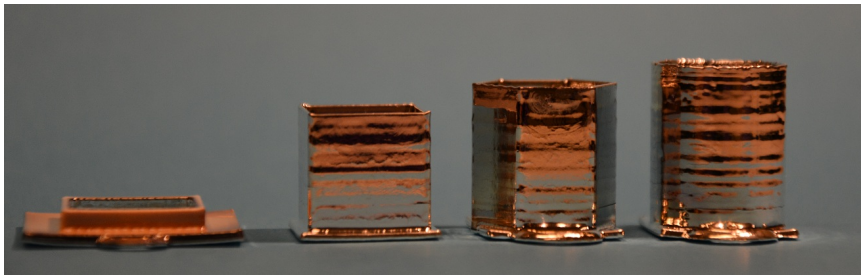

Bachelor's thesis by E.A.P. Marcus

Department of physics and astronomy, group soft condensed matter and nanophotonics

Supervisors: L. van Dijk, M. Sc., Dr. M. Di Vece

Contents

1 Introduction

A major efficiency loss in solar cells is caused by low absorption of light, especially of the long wavelengths. Light partly reflects when hitting the top contact coverage or the front or rear surface of the cell. Optical losses can be reduced in several ways [5], such as minimising top contact coverage, applying anti-reflection coatings, surface texturing [12] (to increase the optical path length internally) or by making cells thicker. However, anti-reflection coatings lead to extra surface recombination and surface texturing has the drawbacks of deteriorating the solar cell quality, increasing parasitic absorption and being limited to high-refractive index materials [11]. Thicker cells, on the other hand, lead to increased costs and more material is used, while the voltage of the cell decreases due to increased recombination[9].

An alternative way to increase absorption in solar cells is adding an external light-trap to the solar cell. Light-trapping can increase the theoretical efficiency limit from roughly 30% to 35% [3], by improving solar cell absorption. The trap enhances the optical path length of the light; this makes it possible to produce thin, but efficient cells. The absorption is improved without increasing recombination. This concept is most interesting at long wavelengths, where solar cells reflect relatively much light but are still efficient. It is beneficial for all solar cells.

We first show how a parabolic concentrator can be used to trap light. Then, we present square, hexagonal and circular concentrator designs. These shapes were chosen because they are suitable to arrange in an array, which is more economical. We calculate several characteristics of the three arrays. Then, we estimate the concentrator transmissions, the absorption of the solar cell with a trap on it and the optical path length enhancement. Following this, we elaborate on the making of silver-coated trap samples with a 3D-printer.

To compare the three concentrators, we performed I-V and spectral response measurements of an organic solar cell with and without 3-D-printed traps on it. The I-V measurements show a decrease in current as compared to the bare cell when the traps are placed on it. However, the spectral response measurements show an increase in efficiency.

2 Parabolic light-traps[1]

A high theoretical efficiency gain by limiting the light emission angle has been calculated [8]. By using the concept of *parabolic concentrators*, we can trap light by this reduction of the emission angle [10].

On the left side of figure 1 such a concentrator on a solar cell is illustrated. The sunlight[2] is focused into the focal point of the parabola (in the figure, we drew three of these rays). The parabola is truncated at a height h and its focal distance is f. The distance between the solar cell and the height where it is cut off is L (L should be bigger than f for better light-trapping).

On the right side of figure 1, two concentrators were placed next to each other. After being reflected by the parabolic concentrator, light rays can hit the bottom of the light-trap and are redirected at the solar cell. Whereas on a bare solar cell any reflected light is lost due to the effects described in section 1, the light-trap recycles some of the reflected light.

2.1 The compound parabolic concentrator (CPC)

It should be noted that the biggest enhancement resides in the first intervals of the light-trapping, as the reflections decay exponentially (see section 2.5). A *compound parabolic concentrator* (CPC) is made by combining two parabolas (see the left side of figure 2). It has two focal points that can be positioned under the trap (see the right side of figure 2). This results in more light hitting the trap than in the ordinary parabolic concentrator, especially for those first important reflections. The distance at which the parabolas are displaced, is indicated by d.

[1] This idea has been explored by Welford [10].

[2] We ignore the angular diameter of the sun and assume that the cell is directed at the sun.

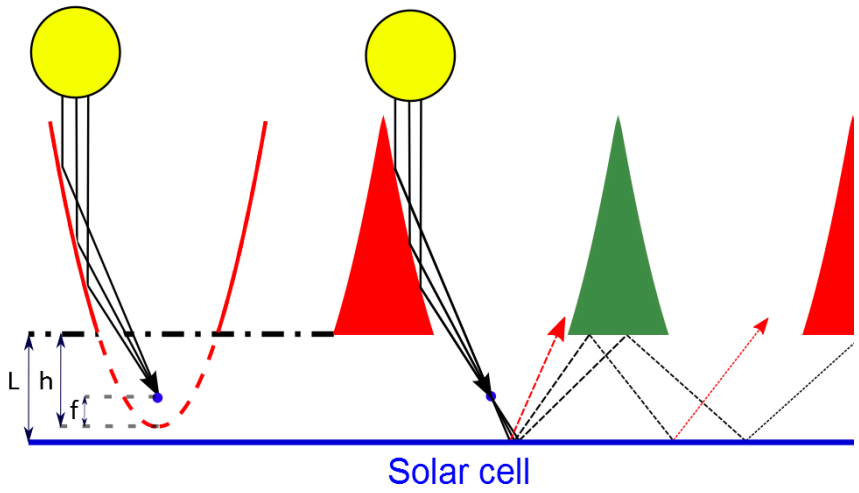

Figure 1: Side view: light-trapping with parabolic concentrators.
(Left) A parabolic concentrator placed above a solar cell. The sunlight is focused into the blue focal point. The dashed part of the parabola is cut off.
(Right) The light rays reflected by the concentrator may hit the solar cell multiple times, resulting in a longer optical path length than on the bare solar cell.

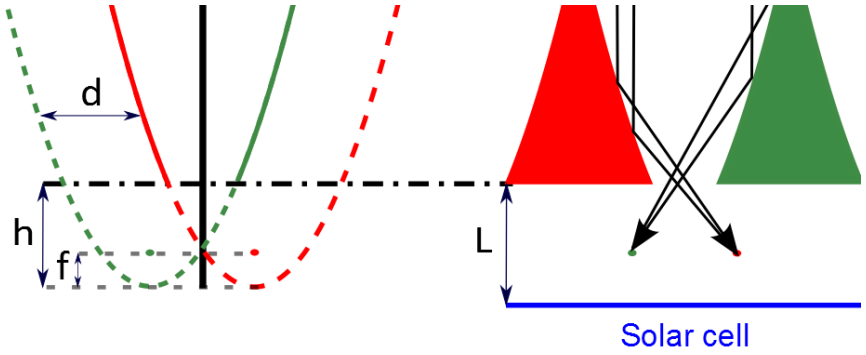

Figure 2: Side view: the compound parabolic concentrator is made by combining to parabolas (left). The CPC doesn't use the dashed part of the parabolas. Light is focused into two focal points (right).

2.2 CPC designs

By extruding the design of section 2.1, we can make a *two-dimensional CPC*, which would look like figure 3(a). Combining two or three of these 2D-CPC's a *square* or *hexagonal CPC* is made, as in figure 3(b) and 3(c). A *circular CPC* can be made by rotating the CPC around its center axis, see figure 3(d). The hole in the bottom of these CPC's is the *aperture*.

We can calculate how much light is trapped by our light-traps. On an untextured solar cell, any light falling directly through the aperture of the CPC still hits the cell perpendicularly and any reflection is lost. However, light hitting the concentrator reaches the cell at an angle with respect to the normal and some reflections are recycled. The fraction of reflected light that is recycled, is

$$t = \frac{CPC\ Area}{Aperture\ Area}$$

the *light-trapping factor*[3].

[3]A two-dimensional CPC with the same height as a square, hexagonal or circular CPC, has a relatively lower light-trapping factor. This makes it less interesting and it is not studied further in this thesis.

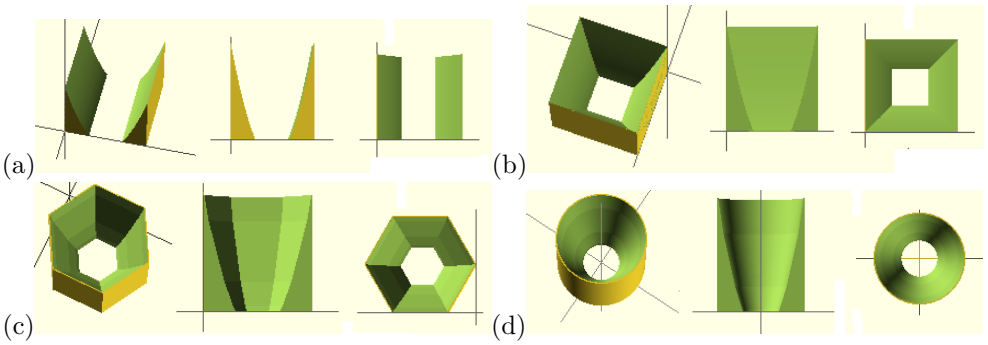

Figure 3: Perspective, cross-section and top view of (a) part of a 2D-CPC and (b) the square, (c) hexagonal and (d) circular CPC.

To compare the square, hexagonal and round CPC's, we fix the focal distance (f), the aperture area (a) and the area of the CPC (A). Keeping A and a constant ensures that every trap receives the same amount of light and determines the light-trapping factor ($t = A/a$).

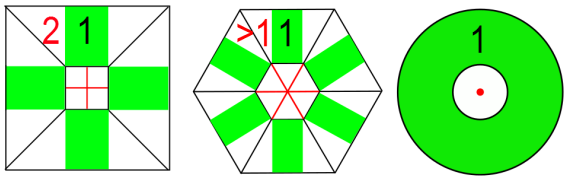

Figure 4: Top view: square, hexagonal and circular CPC's. Only the light hitting the green zones is reflected into the aperture after one reflection. The numbers indicate how many times light is reflected in that region before reaching the aperture. The red lines are the focal lines of parabolic concentrators.

The circular CPC immediately reflects all light into the aperture, but in the square and hexagonal CPC's, this is only accomplished in the green zones in figure 4. Light hitting the CPC in the white zones of figure 4 reflects more than once, leading to optical losses due to the absorption in the CPC and any production imperfections. This can be used to estimate the CPC *transmissions*: the fraction of incident light that reaches the aperture of the CPC (see the appendix for the calculation, section A.1).

2.3 Array considerations

It is more economical to arrange the CPC'ss into an array, because an array has a lower height and is less voluminous[4]. It is easy to arrange the square and hexagonal CPC's into an array. The circular CPC's, need to be stacked in a square or hexagonal order. This results in extrusions, see figure 5. The resulting structure is more fragile and harder to manufacture.

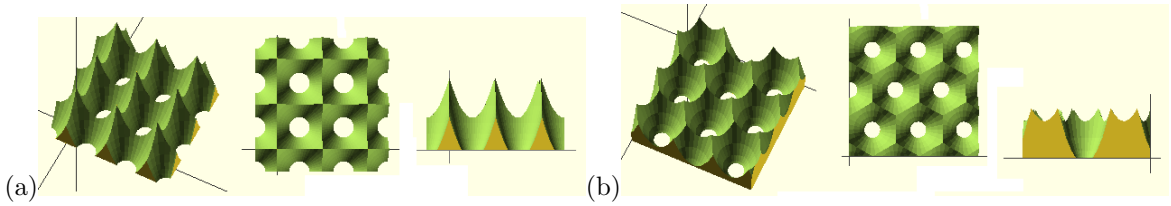

Figure 5: Perspective, top view, cross section: an array of circular conentrators. In (a), the circles are squarely stacked, in (b) hexagonally.

In table 1 we see that the square CPC's form the lowest array; the hexagonal CPC's and the hexagonally and squarely packed circular CPC's are, respectively, 1.15, 1.26 and 1.92 times higher.

An array has edges between the individual CPC's, due to the finite precision of any production method. Light hitting these edges does not reach the aperture properly, resulting in optical losses.

[4] A parabola's height scales with the square of its width. E.g., a trap that is twice as narrow, is four times lower.

CPC	array height ($\frac{5 \cdot a}{16 \cdot f}$)	Edge ratio ($\frac{2 \cdot x}{\sqrt{A}}$)
Square	1	1
Hexagonal	1.15	0.93
Circular (packed hexagonally)	1.26	0.93
Circular (packed squarely)	1.92	1

Table 1: The array height and edge ratios of the four arrays. t is set to 6. Everything is normalised to the values of an array of square CPC's. x is the edge thickness of the production method.

Table 1 shows the ratio of this edge area to the area of one trapping element, for an edge thickness x. It shows that the hexagonal arrays have a 1.07 times lower edge ratio than the square arrays.

2.4 Cell absorption with trap

We estimate how much light the solar cell absorbs with a trap on it. Light that finally reaches the aperture firstly hits the bare cell. A ratio α_{bare} (the absorbance of the bare cell) is absorbed, and a ratio R_{bare} is reflected. In first order, the reflected light can be seen as diffuse with a chance t^{-1} of escaping via the aperture, and a probability $1 - t^{-1}$ of staying trapped.

The trapped light hits the bottom of the trap and a part R_{trap} is sent back to the cell. Again, α_{bare} is absorbed and the reflected light has a chance of t^{-1} of escaping via the aperture, etcetera. This process repeats itself until the intensity of the light is negligible. If we call the transmission of the CPC T_{CPC}, the total absorbance is

$$\begin{aligned}
\text{(Light immediately hitting the cell)} &\quad & T_{CPC} \cdot \alpha_{bare} \\
\text{(...and for the second time)} &+ & T_{CPC} \cdot R_{bare} \cdot (1 - t^{-1}) \cdot R_{trap} \cdot \alpha_{bare} \\
\text{(...and for the third time)} &+ & T_{CPC} \cdot R_{bare}^2 \cdot (1 - t^{-1})^2 \cdot R_{trap}^2 \cdot \alpha_{bare} \\
\text{(...etcetera)} &+ & ...
\end{aligned}$$

or, performing the summation of this geometric serie

$$\alpha_{total} = T_{CPC} \cdot \alpha_{bare} \cdot \sum_{n=0}^{\infty} \left[R_{bare} \cdot R_{trap} \cdot (1 - t^{-1}) \right]^n \tag{1}$$

$$= \frac{T_{CPC} \cdot \alpha_{bare}}{1 - R_{bare} \cdot R_{trap} \cdot (1 - t^{-1})} \tag{2}$$

All parameters in this formula are wavelength-dependent, except for the trapping factor t.

2.5 Enhanced optical path length

Once the light has entered the cage, it follows a longer optical path compared to the bare cell. This *optical path length enhancement* is an *external* enhancement and translates to higher absorption. In first order, the *Beer-Lambert law* is a correct description for the light reflections. According to this law, at every reflection, the intensity decays exponentially with the optical path length enhancement factor ($\Pi_{external}$) as a factor of decay:

$$R_{total} = R_{bare}^{\Pi_{external}}$$

We can correct this for the transmission of the CPC

$$R_{total} = T_{CPC} \cdot {R_{bare}}^{\Pi_{external}}$$

Or, rewriting the previous relation,

$$\Pi_{external} = \frac{\log(R_{total}/T_{CPC})}{\log R_{bare}} \tag{3}$$

This expression is wavelength-dependent, like all parameters in it.

3 Measuring the light-trapping

To measure the optical properties of the different light-traps, trap samples have been made from *acrylonitril butadieen styreen* (ABS) using an *Ultimaker 3D-printer* (see figure 6).

Trap designs (made in Open-SCAD[2]) were converted into $\sim 10^5$ print lines by Cura[1], a slicer. The Ultimaker prints the samples on a platform with a printhead (see the inset of figure 6) that extrudes ABS while following those print lines. After printing a layer, the platform moves down and the Ultimaker prints the next layer on top of the previous one. It is crucial to have a good adhesion of the first layer, otherwise the bottom of the trap will not be smooth or the plastic will warp when it cools. To improve the adhesion of the first layer, Scotch 3M Blue Tape 2090 was applied to the platform.

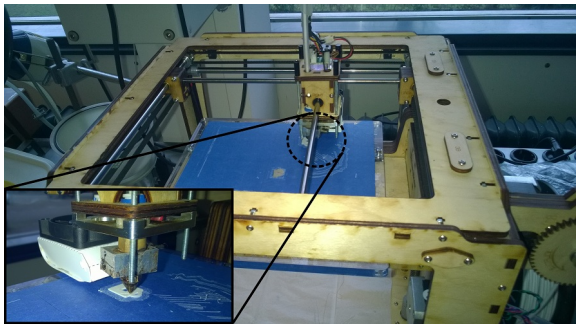

Figure 6: The Ultimaker 3D-printer. On the bottom left, the inset shows a close-up of the printhead, which is printing the first layers of a prototype on the blue tape.

The Ultimaker lacks the precision to attain a smooth finish: the surface of prints is rather rough. Another production imperfection is caused by the plastic contracting when it cools, resulting in slightly curved bottoms (this is called *warping*). When placed on other samples (such as the cages which are described in the next section) or on a solar cell, they leave small openings, through which light can escape.

ABS was chosen as it can be polished with *acetone vapour*. After cooling prints with an icepack, we hold them in a saturated acetone vapour ($T \sim 90°C$) for several seconds, two or three times. The vapour condenses, dissolving the ABS surface, which smoothens. The visual effect of polishing can be seen in figure 7(a).

(a)

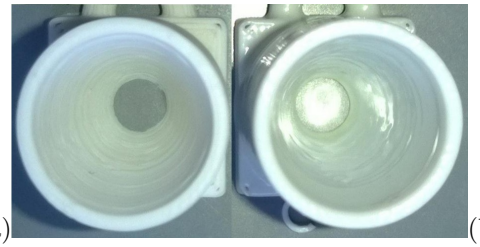

(b)

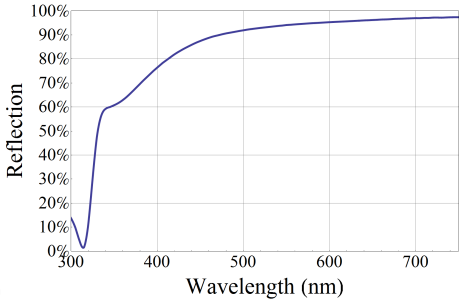

Figure 7: (a) On the left we see an unpolished and on the right a polished sample. (b) The reflection of the used silver layer, as a function of wavelength.

A layer of silver with a thickness of more than 80 nm was sputtered on the traps to guarantee a high reflectivity. The reflection spectrum of the silver layer on aluminium is shown in figure 7(b). At short wavelengths, the silver absorbs a lot of light, almost all of it at 315 nm. At 340 nm, there is more reflection: ~60%. In the long wavelengths, the silver is an excellent mirror, with more than 90% reflection at 460-750 nm.

The light-trapping concept of section 2.1 requires the CPC to be elevated above the solar cell. Square *cages* were made to simulate this. The cages had masks with a side of 25 mm, covering the part of the solar cell (which had an area of 19.7x20 mm^2) we don't use. To make sure any efficiency gains are due to light-trapping and not light concentration, the opening of the square cage has the same area as the CPC. The cage can be seen in figure 8.

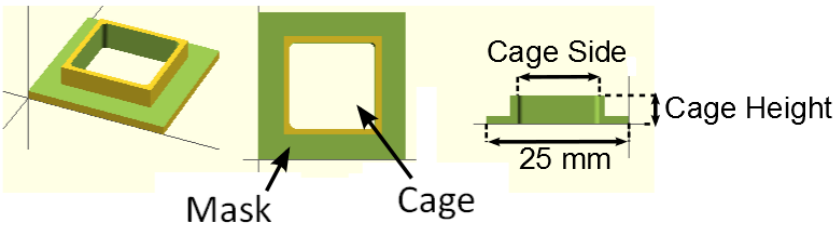

Figure 8: Perspective, top view, cross section: the cage on which concentrators are placed.

Samples for two experiments were made:

1. An experiment to compare the square, hexagonal and round CPC designs, to study the characteristics of a single CPC for use in an array.
2. An experiment to compare a single CPC to a 2x2 array of CPC's.

		a (mm^2)	A (mm^2)	A_{cage} (mm^2)	L (mm)
1. CPC comparison	All designs	35.1	210.4	14.5x14.5	3, 4, 5
2. Array comparison	Single CPC	54	18x18	18x18	12, 16
	2x2 array	13.5(x4)	9x9(x4)	18x18	3, 4

Table 2: A table showing the sizes of the samples.

All traps had a light-trapping factor of 6, a focal distance of 0.7 mm and the parabolas were shifted inwards 0.35 mm (the parameter d of section 2.1). The aperture and CPC areas (a and A), and the area (A_{cage}) and height (L) of the cages can be seen in table 2. The single CPC was four times higher than the array so the its cage needed to be four times as high as the one for the array, to ensure that the light is trapped alike. Of each CPC, two samples were made and of each cage, one. The samples can be seen in figure 9.

(a) 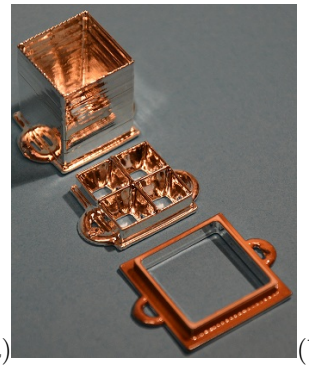 (b) 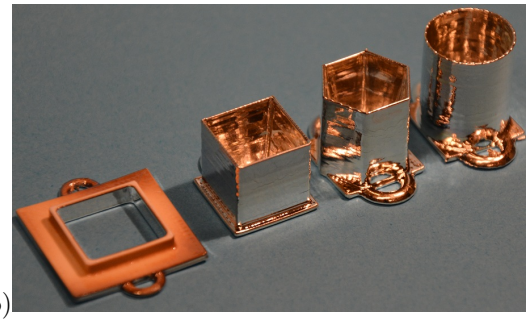

Figure 9: A photo of the samples of experiment (a) 2: the single CPC, the 2x2 array and the cage and (b) 1: the cage, and the square, hexagonal and circular CPC's.

In the first experiment, comparing the square, hexagonal and circular CPC, the aim is to see how the efficiency gains of these different designs compare. Performing the calculation of equations 6, 7 and 5 with $t = 6$ and a constant silver absorption of 5%[5] yields expected transmissions of ~95%, ~93% and ~96%, for the square, hexagonal and circular CPC's (see appendix A.1 for a detailed calculation). Any other losses must be due to printing imperfections.

[5]As can be seen in figure 7, this is reasonable in the region 460-750 nm, but this approximation breaks down in the region 300-460 nm, where the silver has a considerably higher absorption.

In the array experiment, the array will show a lower efficiency gain than the single CPC. This is caused by the extra edges in the middle and the fact that the CPC's in the array are smaller, and as such more prone to imperfections. On top of this, all imperfections are relatively larger compared to the trap and aperture sizes, and have a larger distorting effect. Assuming that all light hitting an edge is lost and a line thickness of 0.1 mm gives an extra loss of ~2% for the array, resulting in a theoretical transmission of ~93%.

3.1 The organic PV-cell

Because the light-trapping mainly improves cell absorption by recycling of reflected light, the effect of the trap is optimal on a cell with a high reflectivity. We used an *organic photovoltaic cell*. Currently, organic cells perform considerably less efficient than silicon cells [4], mainly due to their low optical absorption compared to other cells. They are, however, much cheaper to produce and it is possible to make them large and flexible. Surface texturing is not very effective in organic cells: the maximum path length enhancement that can be achieved by surface texturing is $2n^2$[11] (n is the refractive index of the solar cell material). For crystalline silicon, this amounts to an enhancement factor of 24.5, but this factor is only ~4.5-8 for organic cells, which have a lower refractive index (these values are not reached in practice). External light-trapping is a viable alternative to improve cell absorption.

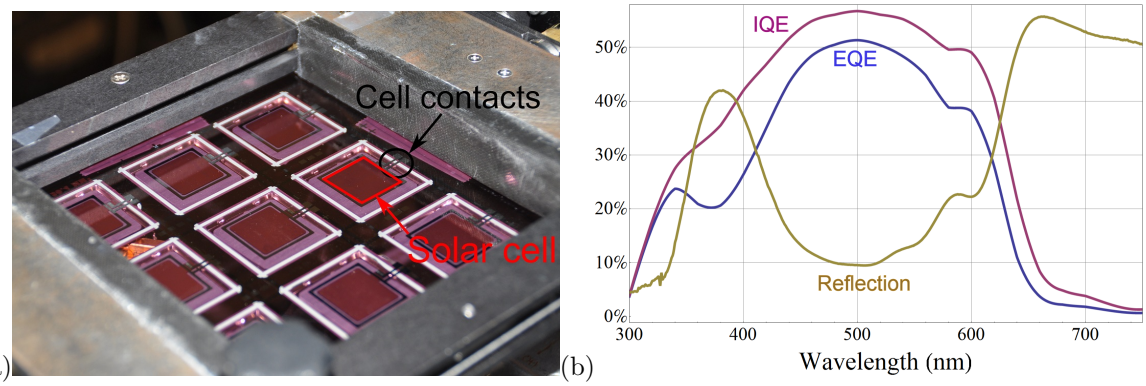

Figure 10: (a) An array of 3x3 of the used organic PV-cells.(b) The *EQE* (blue), *IQE* (mauve) and reflection (yellow) of the bare cell as a function of wavelength.

To determine whether the solar cell (see figure 10) was suitable, we performed a reflection measurement (with an Agilent Cary 5000 setup) and a spectral response measurement. More information about the solar cell can be found in the appendix, see section A.2.

In the spectral response measurement, a light beam is filtered at a certain wavelength. This setup gives the generated electrical current per photon of a certain power in A/W, i.e., it tells us how the solar cell responds to a photon with a certain wavelength. The spectral response measurement was done in intervals of 20 nm, from 300 to 750 nm. The reflection measurement was done in intervals of 1 nm, from 300 to 750 nm.

With the measurement data, the *external* and *internal quantum efficiencies* (*EQE* and *IQE*) of the solar cell were calculated. The *EQE* is the ratio of charge carriers generated to the number of photons of a given energy shining on the cell. It was calculated from the spectral response by

$$EQE = \frac{R_\lambda}{\lambda} \cdot \frac{hc}{e} \approx \frac{R_\lambda}{\lambda} \, (1240\,\mathrm{W \cdot nm/A})$$

with R_λ the spectral responsivity, λ the wavelength, and h, c and e, Planck's constant, speed of light and electron charge.

The *IQE* is the number of charge carriers generated to the number of absorbed photons of a given energy shining on the cell, and can be calculated from the *EQE* as

$$IQE = \frac{EQE}{\alpha_{bare}}$$

with α_{bare}, the absorbance of the bare cell. In figure 10, we plotted the *EQE*, *IQE* and reflection curves of this cell, as a function of wavelength.

Any light-trapping efficiency gain is the highest when the cell has considerable reflection losses and a high quantum efficiency (see equation 4). Looking at the reflection and quantum efficiency spectra (see figure 10), the efficiency gain should be maximal around 400 and 620 nm, where both reflection and efficiency of the cell are high. The trapping effect must first overcome the imperfections created in the production and reflection losses in the trap to achieve a gain. In the region 300-350 nm we expect an efficiency loss: the bare cell absorbs a lot and figure 7 shows that the silver layer on the trap reflects very poorly at these wavelengths.

4 Analysis

The data of the experiment comparing the array and the single CPC showed discrepancies. The single CPC measurements had a very big spread and their mean efficiency was lower than the square CPC used in the first experiment. The two 2x2 array samples had a measured area ratio of ~5 (instead of 6). While these two complications mean that the data for the second experiment aren't representative, the array measurements show that we succesfully made a 2x2 array of square parabolic CPC's. We will now discuss the results of the experiment comparing the square, hexagonal and round CPC designs.

4.1 The electrical measurements

The *I-V* measurements were conducted with an AM1.5G spectrum solar simulator. The voltage was varied in intervals of 0.01 V, from -0.3 V to 0.7 V. Each sample was measured two times. The error in these measurements, even when removing and replacing samples, is very low (~0.03 mA), especially compared to errors introduced by printing imperfections. After each measurement, the sample *and* cage were removed (see figure 12(a) for a photo of a circular sample on the solar cell in this measurement). Thirteen bare cell measurements were done.

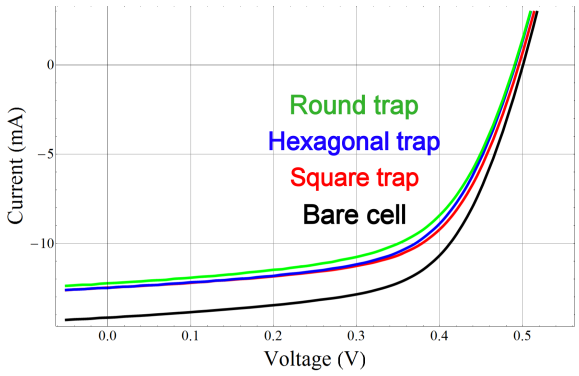

Figure 11: I-V-curves of the bare cell (black), and the cell with the square (red), hexagonal (blue) and circular (green) CPC.

The interesting part of the *I-V*-curves can be seen in figure 11, in which the mean of the two measurement is plotted. The current decreases when the traps are placed on the solar cell. We refrain from concluding anything about how the CPC's compare; the difference in current between them is maximally 0.8 mA. This discrepancy can easily arise because of differences in production imperfections, which cause the largest error.

Surprisingly, the spectral response measurement seems to show a net gain in current; we can explain this in two ways. Firstly, the solar simulator is not a perfect sun; especially in the fact that its solid angle is way bigger than the sun. This causes the light to hit the CPC under a bigger angle than the sun would, which could hinder a part of the light to reach the aperture. Secondly, glass reflections could distort the measurement. When trapped in the cage, the light can still escape by tunneling through the glass.

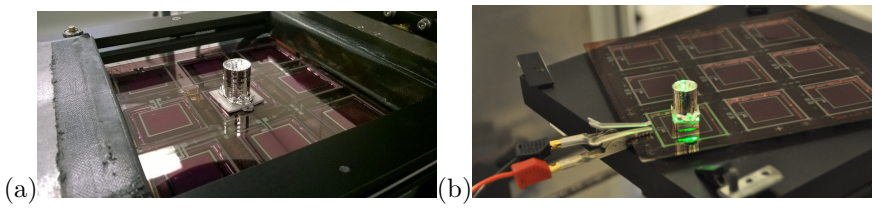

Figure 12: The solar cell with a circular trap on it in (a) an IV measurement and (b) a spectral response measurement.

4.2 CPC transmissions

All spectral response measurements were done from 300 to 750 nm in intervals of 20 nm, with the setup described in section 3.1. For each CPC, two samples were measured, in three measurements (see figure 12(b) for a photo of a measurement with a circular CPC). The cage with height 4 mm was used, which worked best in the IV measurements. The bare cell spectral response was measured six times. Since we only had three spectral response data sets per design, we chose the lowest and highest measurement to be the error bounds. In figure 13 we plotted the measured EQE.

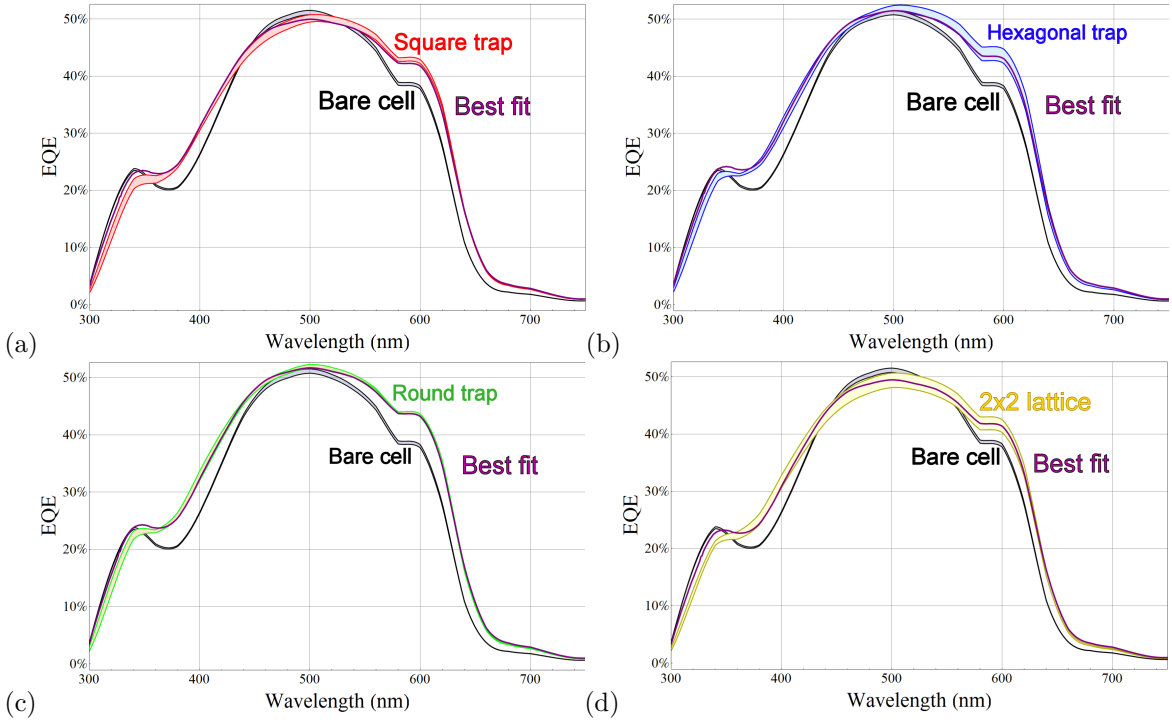

Figure 13: The EQE of the (a) square, (b) hexagonal and (c) round CPC's and the 2x2 array (d). The shaded areas indicate the measurement range. In each graph the bare cell EQE is shown for reference, in black. The purple curves are the best fits.

We can obtain the CPC transmissions by comparing the theoretical absorption to the measurements[6]:

$$\begin{aligned} EQE_{theory} &= IQE_{theory} \cdot \alpha_{total} \\ &\approx IQE_{bare} \cdot \alpha_{total} \end{aligned} \tag{4}$$

[6]We assume that the IQE of the cell is unchanged when a trap is placed on it (i.e. $IQE_{bare} \approx IQE_{with\,trap}$).

with α, the absorption. We can fit the theoretical EQE to the data with relation 1. We have measured R_{bare} and for R_{trap} we can use the silver reflection as presented in figure 7. As such, the only fitting parameter is the CPC transmission, T_{trap} (approximated as constant). The best fits are also in figure 13. The fits are mostly within the measurement range. The model only breaks down in the low-wavelength part of the spectrum (300-360 nm), where the lower silver reflection should result in a decreased CPC transmission.

CPC	Theoretical transmission	Fitted transmission
Square	95%	$(90 \pm 1)\%$
Hexagonal	93%	$(93 \pm 2)\%$
Circular	96%	$(93 \pm 1)\%$
2x2 array	93%	$(89 \pm 2)\%$

Table 3: A table showing the transmissions found by fitting and those calculated with equations 6, 7 and 5.

In table 3, the best fit values[7] for the transmissions are shown next to the theoretically found transmissions of section 3.1. Comparing them, we can conclude that production imperfections cause a transmission loss in the range of $(4 \pm 2)\%$. We can also deduce that in this experiment, it is very likely that the used hexagonal CPC samples were of a higher quality than the circular and square samples. These quality differences could account for the disparity in EQE gain. We can also see that the 2x2 array has a lower transmission than the square CPC, as expected.

4.3 Optical path length enhancement

We also determined the external path length enhancement with expression 3. The total reflection was found with $R_{total} = 1 - \alpha_{total} = 1 - \frac{EQE_{with\,trap}}{IQE_{bare}}$. Here, we again supposed $IQE_{bare} \approx IQE_{with\,trap}$. The measurement range is determined by calculating the enhanced optical path length with the minimum and maximum EQE. The results are plotted in figure 14[8]. $\Pi_{external}$ has the same behaviour as the gain spectrum, which we describe in section 4.4. In the lion's share of the spectrum, there is an improvement as compared to the bare cell in the path length that the light traverses.

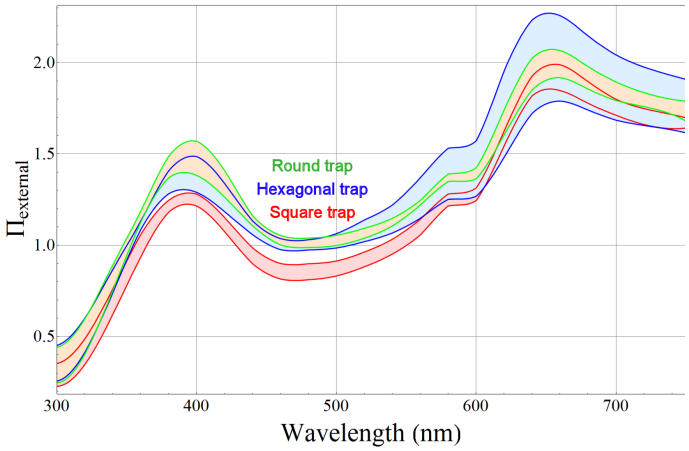

Figure 14: The calculated optical path length enhancements: of the square (red), hexagonal (blue) and circular (green) trap. The shaded areas are the measurement range.

[7] To estimate the error in the found transmission, we also fitted the model to the minimum and maximum measured EQE curves.

[8] The optical path length enhancement for the 2x2 array can be found in the appendix, see figure 17(b).

4.4 The absolute *EQE* gain

For the cell with traps, the measurement range is larger, up to ~2-3% in some regions. We graphed the absolute *EQE* gain with the traps in figure 15[9]. The measurements indicate a gain in external quantum efficiency in almost all of the efficient spectrum, but are not conclusive about which CPC is the best. The *EQE* gains have the same behaviour for the three designs and are significantly distinguishable from the bare cell *EQE*[10].

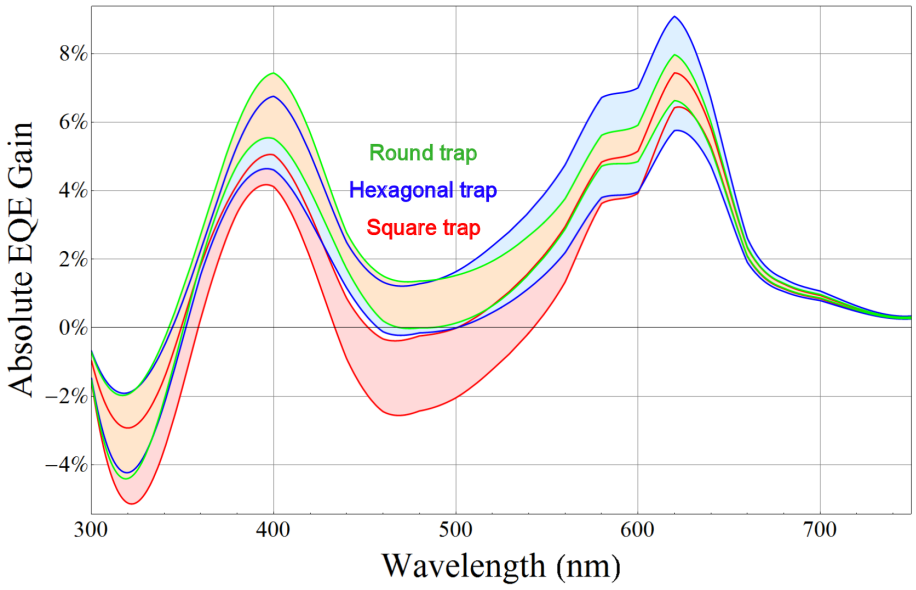

Figure 15: The absolute *EQE* gains compared to the bare cell, of the square (red), hexagonal (blue) and circular (green) CPC's. The shaded regions are the measurement range.

300-350 nm: The loss in this region peaks at $\sim (-3 \pm 1)\%$. This is a loss due to the poor reflection of the silver at these wavelengths and the fact that the cell already absorbs a lot of light without a trap.

350-440 nm: The traps improve efficiency here, as the silver reflection improves and the cell is efficient, but has a high reflection. The gain peaks at 400 nm, with gains of $\sim 4 - 7\%$.

440-520 nm: When the reflection of the cell plummets, so does the trapping gain. On the other hand, the silver reflects the light better here. At 440 nm, the square trap seems to be decreasing quantum efficiency again, with a local minimum of $\sim (-1 \pm 1)\%$, while the hexagonal and circular trap gain $\sim (1 \pm 1)\%$.

520-750 nm: The gain starts rising again at 500 nm, following the cell reflection. At 580-600 nm, we quite clearly see a plateau: this is the same plateau as in the cell reflection curve! The gain has another peak at 620 nm. Here, its maximum is $\sim (7 \pm 2)\%$. Afterwards, the quantum efficiency of the solar cell falls, and the trapping gain with it.

We clearly see the effects as expected in section 3.1. We understand the physical mechanisms involved; most importantly, light-trapping is a means to reduce reflections. The trapping gains follow the trend of the reflection curve of the solar cell.

In the comparison of the three designs, this data set is only conclusive from ~375 to 500 nm. There, the square CPC has a lower efficiency gain than the round CPC. From ~450 to 500, the square CPC also has a lower efficiency gain than the hexagonal CPC. This happens because the transmission of the square CPC samples was lower than the transmissions of the hexagonal and round samples (see table 3).

[9]The EQE gain of the array can be found in the appendix and is alike to the gain with the square trap, albeit slightly lower, see figure 17(a).

[10]As the graph neatly follows the solar cell's reflection and its efficiency, it is useful to have a look at figure 10 again.

5 Discussion

We showed that light traps made with square, hexagonal and circular CPC's improved solar cell efficiency. To see how these light-traps perform on cells with different reflection characteristics, this research should be repeated on other solar cells. Our model can help in this research. In future research the *EQE* curves can be integrated with a solar spectrum to calculate if there is a net gain when the cell is exposed to sunlight. Alternatively, this could also be solved by doing the measurements outside, in direct sunlight. The measurement to compare a single trap to a 2x2 array should also be repeated, to see how much optical loss is created by arranging traps into an array. The trap transmissions can also be measured directly. Other measurements, like an absorption measurement of the cell with a trap on it, can be done as well. Our theory can be refined: especially in treating the transmission of the traps as wavelength-independent. The transmission should be joined to the silver reflection spectrum, to increase the fitting quality of our model, which lacks precision in the short wavelength region.

With a ray tracer for light-trapping, the focal distance and inward shift of the parabola side can be optimized. In addition to this, the angle of acceptance of the trap can be determined. This would be useful to design a trap that makes tracking unnecessary.

There are some drawbacks to light-traps. In section 3 we elaborated on two causes of optical losses: the imperfect reflection of silver and production imperfections. Additionally, light hitting the trap will enter the cell under an angle with respect to the normal. This reduces efficiency, because solar cells absorb light better if it hits them perpendicularly[7].

The biggest flaw in this research, is still the production of the traps. This caused the comparison of the CPC's to be inconclusive. The Ultimaker 2, which has a heated print-bed, or other 3D-printers (for example MakerBot) or materials (e.g. resin) may have a higher sample precision. Other production methods can also be tried (like milling or injection molding).

When the best candidate for light-trapping is established, mass production methods should be found. Furthermore, we need to know if this concept warrants its production. Does the gain in solar cell efficiency outweigh the production costs? And how does this gain compare to other possible gains, like surface texturing?

Light-traps can be combined with tandem solar cells. In such a solar cell, the top layer should be efficient in the long-wavelength part of the spectrum. This layer gains a lot from the light-trapping. At short wavelengths, light-trapping would lead to a loss (due to the poor silver reflection), but short wavelengths are absorbed by the bottom layer.

To keep the light optimally trapped, it should be reflected specularly, as any diffuse reflection can lead to escape. As the light intensity decays exponentially (see section 2.5), this is especially important for the first passages. The highest light-trapping gain should, accordingly, be seen for a specularly reflecting cell. Ultimately external light-trapping could be better than surface texturing, because a flat cell design also has a superior electrical quality[9].

External light-trapping is beneficial for all solar cells and the parabolic light-traps as they are presented in this thesis result in a higher quantum efficiency!

6 Conclusion

We have shown how to make square, hexagonal and circular light-traps with parabolic mirrors. These external light-traps are designed to improve light absorption of solar cells. We first concluded that the square trap had geometrical advantages; it has a lower height and is less complex. Measurements showed a gain in quantum efficiency in almost all of the spectrum and we succesfully made a 2x2 array of traps.

The traps were 3D-printed and coated with silver and their effects on an organic solar cell were measured. While *I-V* measurements seemed to indicate a current loss when the traps are placed on the cell, the spectral response of the solar cell, which we deem more reliable, shows that the quantum efficiency is higher with traps. Unfortunately, the spread in production accuracy was high, which limited us in the comparison of the three designs. It does show that we succesfully made a 2x2 array of parabolic light-traps, with a slightly lower transmission than the individual traps. The

3D-printer made samples with slightly curved tops and bottoms, resulting in more optical losses because light can escape through openings between the cage and solar cell or cage and CPC.

We analysed this gain spectrum in depth, and we understand the physical mechanisms involved. The key ingredients for understanding the light-trapping are the spectra of the silver reflection and the solar cell reflection and efficiency. The trap improves the efficiency of the solar cell where the cell reflects relatively much, but is efficient. At short wavelengths, silver reflects poorly, leading to an efficiency loss with silver-coated traps. On this organic solar cell, this resulted in a peak efficiency loss of ~3% at 320 nm and peak efficiency gains of ~5% and ~7% at 400 and 620 nm.

By fitting the external quantum efficiencies to the theoretical absorption, the CPC transmissions were derived. We compared these transmissions to their theoretical estimate, and calculated that $\sim(4 \pm 2)\%$ of the intensity was lost due to 3D-printing imperfections. We also calculated the optical path length enhancement; disregarding the short wavelengths (300-350 nm), the traps increase the path length of light rays, improving the chances for the light to be absorbed.

Acknowledgements

I would like to thank Lourens van Dijk and Marcel Di Vece for their supervision and help. I am also grateful to Jolt Oostra and TNO for the organic photovoltaic cells and Amolf for the use of their silver sputter tool.

Furthermore, I acknowledge the help of Klaas Bakker from ECN (with the spectral response measurement) and Gerhard Blab (with the 3D-printer).

References

[1] Cura, slicer software. *software.ultimaker.com*, 2014.

[2] Openscad, cad software. *www.openscad.org*, 2014.

[3] Patrick Campbell and Martin A Green. The limiting efficiency of silicon solar cells under concentrated sunlight. *Electron Devices, IEEE Transactions on*, 33(2):234–239, 1986.

[4] Shi-Wen Chiu, Li-Yen Lin, Hao-Wu Lin, Yi-Hong Chen, Zheng-Yu Huang, Yu-Ting Lin, Francis Lin, Yi-Hung Liu, and Ken-Tsung Wong. A donor–acceptor–acceptor molecule for vacuum-processed organic solar cells with a power conversion efficiency of 6.4%. *Chemical Communications*, 48(13):1857–1859, 2012.

[5] C. Honsberg and S. Bowden. Optical losses. *http://pveducation.org/pvcdrom/design/optical-losses*, 2014.

[6] A Jolt Oostra, Paul WM Blom, and Jasper J Michels. Prevention of short circuits in solution-processed oled devices. *Organic Electronics*, 15(6):1166–1172, 2014.

[7] David L King, Jay A Kratochvil, and William E Boyson. Measuring solar spectral and angle-of-incidence effects on photovoltaic modules and solar irradiance sensors. In *Photovoltaic Specialists Conference, 1997., Conference Record of the Twenty-Sixth IEEE*, pages 1113–1116. IEEE, 1997.

[8] Emily D Kosten, Jackson H Atwater, James Parsons, Albert Polman, and Harry A Atwater. Highly efficient gaas solar cells by limiting light emission angle. *Light: Science & Applications*, 2(1):e45, 2013.

[9] Hitoshi Sai, Yoshiaki Kanamori, and Michio Kondo. Flattened light-scattering substrate in thin film silicon solar cells for improved infrared response. *Applied Physics Letters*, 98(11):113502, 2011.

[10] Walter Thompson Welford. *High collection nonimaging optics*. Elsevier, 2012.

[11] Eli Yablonovitch. Statistical ray optics. *JOSA*, 72(7):899–907, 1982.

[12] Jianhua Zhao, Aihua Wang, Martin A Green, and Francesca Ferrazza. 19.8% efficient honeycomb textured multicrystalline and 24.4% monocrystalline silicon solar cells. *Applied Physics Letters*, 73(14):1991–1993, 1998.

A Appendix

A.1 CPC transmissions

The CPC transmissions were calculated as follows: the CPC area is A and the aperture area a and we assume that α_{trap} (the absorbance of the trap) of the light intensity is parasitically absorbed upon a reflection. Any light passing through the aperture (a fraction a/A) reaches the cell without reflections. In a *circular CPC*, all other light reaches the aperture after one reflection, thus the absorption loss in the trap (L) can be estimated as

$$L_{circular\,CPC} = \alpha_{trap} \cdot \frac{1}{A} \cdot (A - a) = \alpha_{trap} \cdot (1 - t^{-1})$$

with the identity $a/A = t^{-1}$. The fraction of light that reaches the aperture without being absorbed (the *transmission,T*) is one minus this loss,

$$T_{circular\,CPC} = 1 - \alpha_{trap} \cdot (1 - t^{-1}) \tag{5}$$

In the *square CPC*, the light hitting the green zones of figure 4 reaches the aperture upon one reflection. These green zones have an area of $2 \cdot (\sqrt{A \cdot a} - a)$, leading to a loss of

$$L_{one\,reflection} = \alpha_{trap} \cdot \frac{1}{A} \cdot 2 \cdot (\sqrt{A \cdot a} - a)$$

Any light hitting the zones of the CPC not marked green is directed to a focal line. In first order, it hits a green zone at the next reflection, and thus reaches the aperture in two reflections (leading to a loss of $\alpha_{trap} + \alpha_{trap} \cdot R_{trap} \approx 2 \cdot \alpha_{trap}$[11]). The loss is

$$L_{two\,reflections} = 2 \cdot \alpha_{trap} \cdot \frac{1}{A} \cdot (A + a - 2 \cdot \sqrt{A \cdot a})$$

Replacing a/A by t^{-1}, the transmission of the square CPC is one minus these losses,

$$T_{square\,CPC} = 1 - 2 \cdot \alpha_{trap} \cdot (1 - t^{-1/2}) \tag{6}$$

In the *hexagonal CPC*, the green zones have an area of $2 \cdot (\sqrt{A \cdot a} - a)$. Light in these zones reflects one time, leading to a loss of

$$L_{one\,reflection} = \alpha_{trap} \cdot \frac{1}{A} \cdot 2 \cdot (\sqrt{A \cdot a} - a)$$

The zones of more reflections have an area of $A + a - 2 \cdot \sqrt{A \cdot a}$. If we assume that light reaches the aperture after a mean of 2.5 reflections when hitting these zones, they will lead to a loss of

$$L_{?\,reflections} = 2.5 \cdot \alpha_{trap} \cdot \frac{1}{A} \cdot (A + a - 2 \cdot \sqrt{A \cdot a})$$

The transmission of the hexagonal CPC is one minus these losses,

$$T_{hexagonal\,CPC} = 1 - 2.5 \cdot \alpha_{trap} - 3 \cdot \alpha_{trap} \cdot t^{-1/2} + 0.5 \cdot \alpha_{trap} \cdot t^{-1} \tag{7}$$

[11] This is only correct if R_{trap} is sufficiently close to 1; which is fair for silver, see figure 7.

A.2 The organic photovoltaic cell

The used organic PV-cells were made by spin-coating PEDOT:PSS on a glass substrate with nine ITO pixels. On this layer, P3HT:PCBM was spin-coated and lithium fluoride and aluminium were applied. The substrates were then encapsulated with a metal lid to prevent oxidation. A more detailed version of the process-method can be found in section 2.2 of Oostra, 2014 [6] (with P3HT:PCBM instead of LEP and a one nm LiF layer instead of a 5 nm Ba layer). A schematic figure of the solar cell can be seen in figure 16

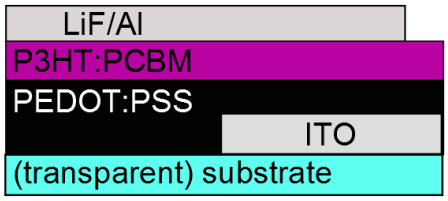

Figure 16: The OPV-cell.

A.3 2x2 array

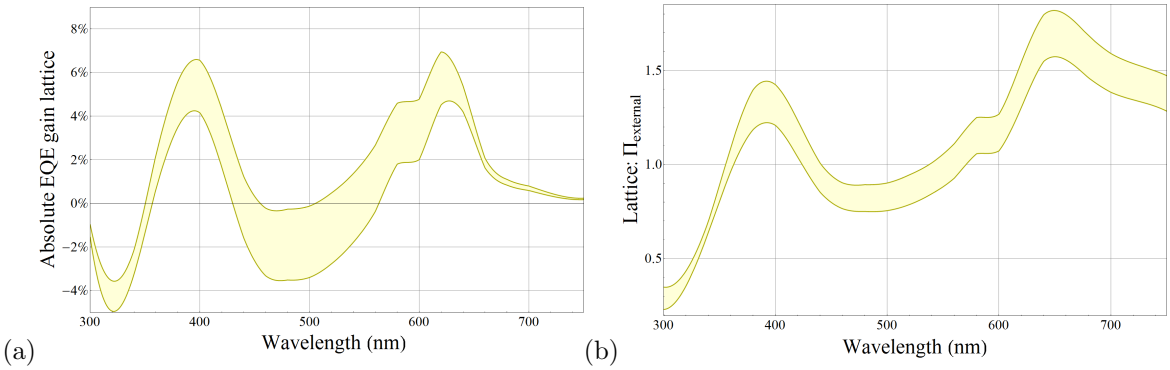

(a) (b)

Figure 17: The absolute EQE gain (a) and the optical path length enhancement (b) of the 2x2 array.